

Quantum statistical imaging of particles without restriction of the diffraction limit

Jin-Ming Cui, Fang-Wen Sun,* Xiang-Dong Chen, Zhao-Jun Gong, and Guang-Can Guo
Key Lab of Quantum Information, University of Science and Technology of China, Hefei 230026

(Dated: October 10, 2012)

A practical quantum measurement method based on the quantum nature of anti-bunching photon emission has been developed to detect single particles without the restriction of the diffraction limit. By simultaneously counting the single-photon and two-photon signals with fluorescence microscopy, the images of nearby Nitrogen-Vacancy centers in diamond at a distance of 8.5 ± 2.4 nm have been successfully reconstructed. Also their axes information was optically obtained. This quantum statistical imaging technique, with a simple experimental setup, can also be easily generalized in the measuring and distinguishing of other physical properties with any overlapping, which shows high potential in future image and study of coupled quantum systems for quantum information techniques.

PACS numbers: 06.30.Bp, 42.30.Wb

The measurement of physical quantities is not only a major goal but also an active impulsion for scientific research. Especially, the imaging of nearby particles is important for modern science [1, 2]. The precision with which two nearby particles can be resolved is classically restricted by the optical diffraction limit. Imaging methods that use distinguishing information based on the photons emitted from the different particles have been proposed to achieve precision beyond the diffraction limit [3–9]. When the emitted photons have the same properties, distinguishing nearby particles that are separated by distances much less than the diffraction limit is difficult.

Recently, quantum techniques are being applied to enhance the precision of measurements beyond the classical limit [10, 11]. However, many quantum-based protocols to improve the measurement used the quantum superposition or entanglement. They are fragile because of quantum decoherence and remain at the proof-of-principle stage [12–14]. Here, we have developed a practical quantum measurement method to detect single particles without the restriction of the diffraction limit. In the quantum regime, the situation for particle imaging is different because each particle emits only one photon and shows the single-photon antibunching effect [15]. By detecting the photon coincident counts, the particles can be imaged and resolved even when they are almost completely overlapping and the emitted photons are identical. Here, Nitrogen-vacancy (NV) centers in diamond were used in this experiment to demonstrate the quantum statistical imaging (QSI) method. Single NV center has shown its good quality as a single-photon source [16, 17]. When two NV centers are close to each other, i.e., within tens of nanometers, the strong dipole-dipole interaction can be applied in quantum information techniques [18, 19]. Diamond nano-crystals with NV centers have been successfully used to image biological processes [20, 21]. The ability to image and distinguish two nearby NV centers is becoming increasingly important in physics [18, 19, 22] and biology [20, 21].

NV centers are usually detected by scanning confocal optical fluorescence microscopy [23], in which the single-photon intensity of spontaneous emission is measured to characterize the optical images of the centers. A home-built confocal scan-

ning microscopy was used to image single NV centers which were fabricated by nitrogen ions implantation. The spontaneous emission of photons from the NV centers is collected into a single-mode fiber. The collected photons are then split into two paths by a fiber beam splitter with a transmissivity of T and a reflectivity of R ($T + R = 1$). Finally, the separated beams are detected with two single-photon detectors. When two NV centers (A and B) are imaged, the single-photon intensity at position (x, y) from the single-photon detectors D_1 and D_2 can be expressed as

$$\begin{aligned}\langle I_1^{D1}(x, y) \rangle &= T[\langle I_A(x, y) \rangle + \langle I_B(x, y) \rangle], \\ \langle I_1^{D2}(x, y) \rangle &= R[\langle I_A(x, y) \rangle + \langle I_B(x, y) \rangle],\end{aligned}$$

where $\langle I_A(x, y) \rangle$ and $\langle I_B(x, y) \rangle$ are the single-photon rates from NV centers A and B , respectively. Therefore, the single photons from the two NV centers are

$$\begin{aligned}\langle I_1(x, y) \rangle &= \langle I_1^{D1}(x, y) \rangle + \langle I_1^{D2}(x, y) \rangle \\ &= \langle I_A(x, y) \rangle + \langle I_B(x, y) \rangle.\end{aligned}\quad (1)$$

When the distance between the two NV centers is within the optical diffraction limit, $\langle I_A(x, y) \rangle$ and $\langle I_B(x, y) \rangle$ are overlapping and hardly distinguishable from the single-photon intensity $\langle I_1(x, y) \rangle$. If two-photon coincident counts are measured, then the two photons must come from two NV centers and never from the same NV center because a single NV center only emits one photon. This attribute demonstrates a genuine quantum characteristic, namely, the photon antibunching effect with $\langle [I_A(x, y)]^2 \rangle = \langle [I_B(x, y)]^2 \rangle = 0$. Therefore, the two-photon intensity will be

$$\langle I_2(x, y) \rangle = \eta_2(1 + K)RT \langle I_A(x, y) \rangle \langle I_B(x, y) \rangle, \quad (2)$$

where η_2 is the two-photon detection constant, which is based on the imperfections resulting from the photon collection efficiency, path loss, detection efficiency of the single-photon detectors and detection windows in the experiment. In the above equation, K describes the quantum

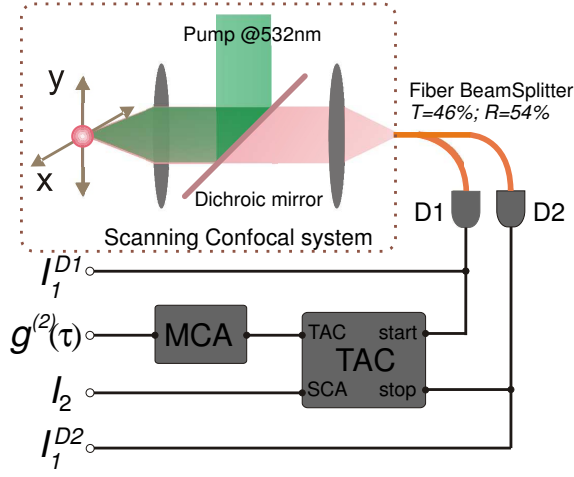


FIG. 1: (color online) Schematic of measurement setup. Confocal NV fluorescent photons are splitted by a fiber beam splitter with splitting ratio of 46 : 54 and sent to single photon detector $D1$ and $D2$. TAC is used to get coincidence counts of $D1$ and $D2$ from SCA output, while TAC output is connected to a MCA to implement autocorrelation measurement ($g_c^{(2)}(\tau)$). I_1^{D1} , I_1^{D2} , and I_2 are $D1$, $D2$ and coincidence count rates, respectively.

indistinguishability-induced bunching effect of the two photons [24, 25]. Usually, $K = 0$ in many measurements without special spectral filtering. For example, the photon from NV center in diamond has very broad phonon bandwidth comparing to its narrow zero-phonon line width [23], leading $K = 0$ in the present measurement. Therefore, simply from $\langle I_1(x, y) \rangle$ and $\langle I_2(x, y) \rangle$, the values of $\langle I_A(x, y) \rangle$ and $\langle I_B(x, y) \rangle$ can be obtained, even if the two particles are completely overlapping. Subsequently, the optical images of the two NV centers can be reconstructed and distinguished. For N particles, m -th ($1 \leq m \leq N$) order coincidence measurement will give

$$\langle I_m(x, y) \rangle = \eta_m \sum [\langle I_A(x, y) \rangle \langle I_B(x, y) \rangle \dots]_{m \text{ different points}},$$

where η_m is the m -photon detection constant and the photon indistinguishability induced photon bunching effect is also neglected. There are N independent values, where images of each particles can be solved and reconstructed. Here there is no need to have any assumption on the distribution function of the image or the point spread function [26]. This technique utilizes a genuine quantum phenomenon to produce this result without classical parallelism.

In the experiment, the NV centers are excited by a 532 nm green laser, and the emitted fluorescence is acquired with a laser scanning confocal microscope and sent to the Hanbury-Brown-Twiss interferometer [27], as shown in Fig. 1. The collected photons are split and sent to two single-photon detectors $D1$ and $D2$, whose single-photon counting rates are recorded as $\langle I_1^{D1} \rangle$ and $\langle I_1^{D2} \rangle$. To record the two-photon counting rate $\langle I_2 \rangle$ at the same time, a single-channel analyzer (SCA) on a time-amplitude converter (TAC) is used to obtain

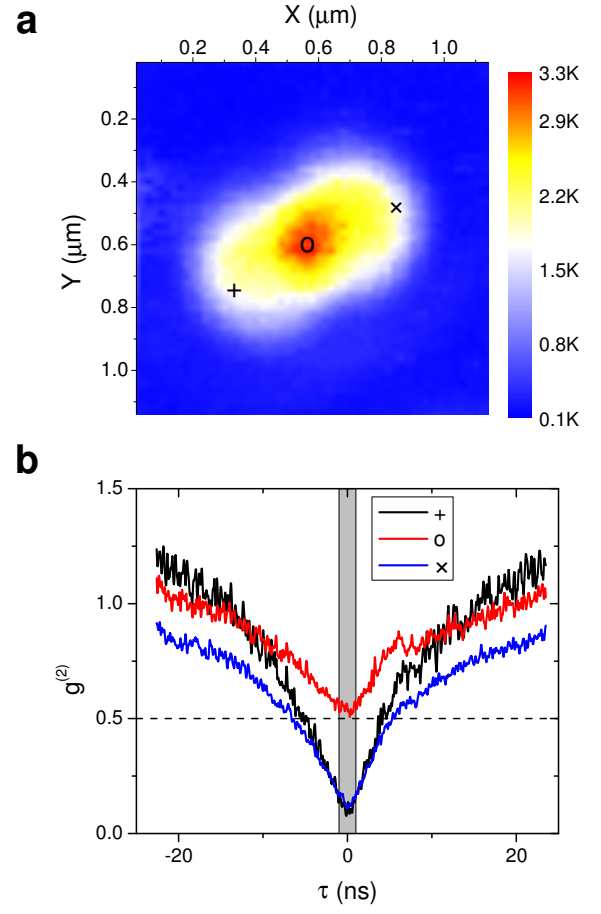


FIG. 2: (color online) (a) Confocal image of two NV centers apart from 366.1 nm, which is at the resolution of confocal measurement. (b) $g_c^{(2)}(\tau)$ at different points in (a). See the text for more details. The gray window indicates the SCA window $t_w = 2$ ns to measure I_2 .

the coincidence counts of $D1$ and $D2$, with a SCA window width of $t_w = 2$ ns at $\tau = 0$ because a single NV center has an anti-bunching decay with a width of approximately 20 ns. The two-photon autocorrelation measurement ($g_c^{(2)}(\tau)$) is performed by the multi-channel analyzer (MCA). Using scanning confocal microscopy, $\langle I_1 \rangle = \langle I_1^{D1} \rangle + \langle I_1^{D2} \rangle$ and $\langle I_2 \rangle$ for each position are recorded to construct single-photon and two-photon images. The coincidence measurement is conducted in start-stop mode in the TAC, and

$$\eta_2 = \frac{2t_w \langle I_1^{D1} \rangle \langle I_1^{D2} \rangle}{RT(\langle I_1^{D1} \rangle + \langle I_1^{D2} \rangle)^2}$$

with $R = 54\%$ and $T = 46\%$.

Two nearby two-NV-center pairs were measured. Fig. 2 (a) displays a confocal scanning image of the first two-NV-center pair. The position with maximal intensity marked as “o” is at the overlapping area of two NV centers. If confocal spot is fixed on this position, both NV centers are excited in the pump focus with $g_c^{(2)}(0)$ about 0.5. However, while the confocal spot is on side position marked as “+” or “x”, only

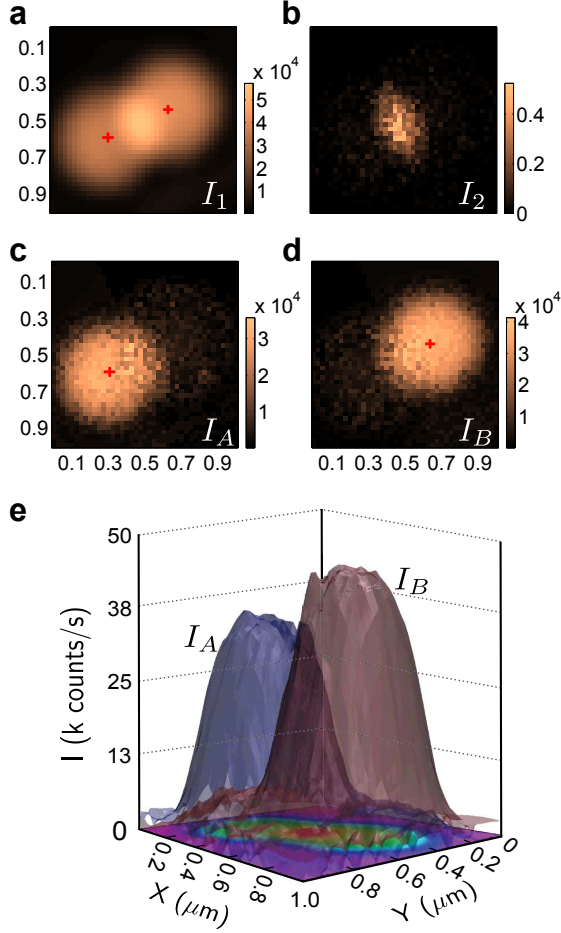


FIG. 3: (color online) Optical images of two single NV centers at a distance of 366.1 ± 2.8 nm. (a) and (b) show I_1 and I_2 for the single-photon and two-photon counting, respectively, and (c) and (d) are images of each NV center (I_A , I_B) obtained from Eq.(1) and (2) for each pixel with measured I_1 and I_2 data, respectively. The red crosses mark the positions of the NV centers with an uncertainty of $1/20$ the length of each cross. The positions were obtained using a two-dimensional (2D) Gaussian fitting of I_A or I_B . (e) A 3D image of the two NV centers.

one NV center are effectively excited as another NV center is out of exciton spot. Therefore, $g_c^{(2)}(0)$ is close to zero as a single NV center. Fig. 2 (b) displays $g_c^{(2)}(\tau)$ which has removed noise. From marked positions “+” to “o” in Fig. 2 (a), it is clear to see the variation from single to double NV centers.

For the first pair, the single-photon intensity ($\langle I_1(x, y) \rangle$) and two-photon intensity ($\langle I_2(x, y) \rangle$) were recorded at the same time (Fig. 3 (a, b)). In Fig. 3 (b), the image of the two-photon intensity has a narrower width in the overlapping region of the two NV centers. However, this image does not provide spatially resolved images of the two NV centers. The image of a single NV center should have a single peak and a continuous envelope. Using $\langle I_1(x, y) \rangle$ and $\langle I_2(x, y) \rangle$, the photon intensities $\langle I_A(x, y) \rangle$ and $\langle I_B(x, y) \rangle$ of the two par-

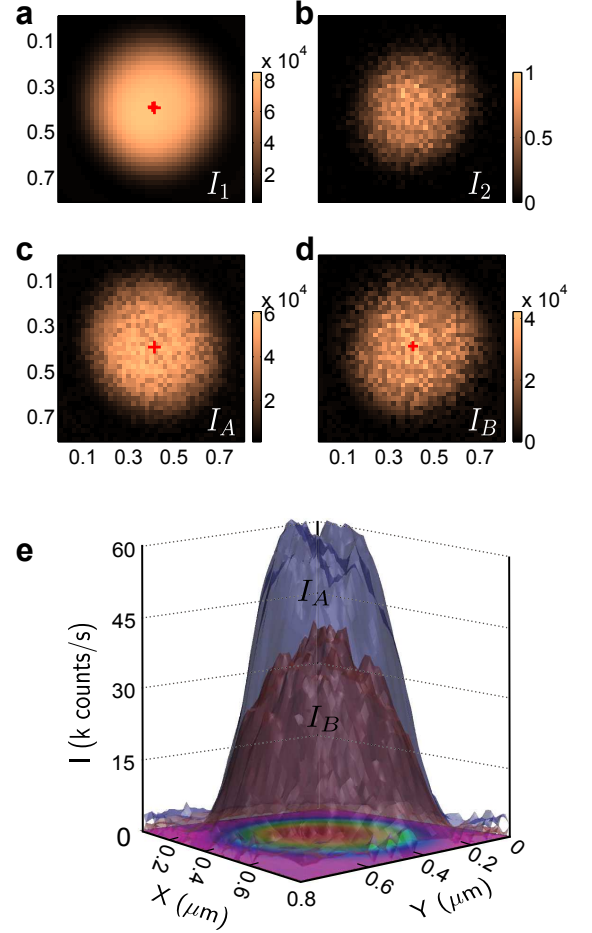


FIG. 4: (color online) Optical imaging of two single NV centers with a small separation. The images are organized as in Fig.3. The distance between the NV centers was determined to be 8.5 ± 2.4 nm by fitting I_A and I_B . This distance is much smaller than the diffraction limit.

ticles can be obtained by solving Eq. (1) and Eq. (2). The images of the two particles, I_A and I_B , were reconstructed and are shown in Fig. 3(c, d). By fitting the data, the distance between the centers was determined to be 366.1 ± 2.8 nm, which is at the edge of the diffraction limit. Fig. 3 (e) shows a three-dimensional (3D) image of the two nearby NV centers, and the overlapping of the NV centers can be observed.

Another pair of NV centers with a much smaller separation was also measured and distinguished with the QSI method. The confocal scanning image, the result of photon autocorrelation measurement and the spectrum show that there are two NV centers (see Supplementary Figure S2). The single-photon and two-photon images are shown in Fig. 4 (a, b). Based on the single-photon intensity, the two NV centers are well overlapping and cannot be distinguished. Using the QSI method, their images, I_A and I_B , can be obtained, shown in Fig. 4 (c, d). The distance between the centers was determined to be 8.5 ± 2.4 nm by fitting I_A and I_B . This distance is much smaller than the diffraction limit, and the NV cen-

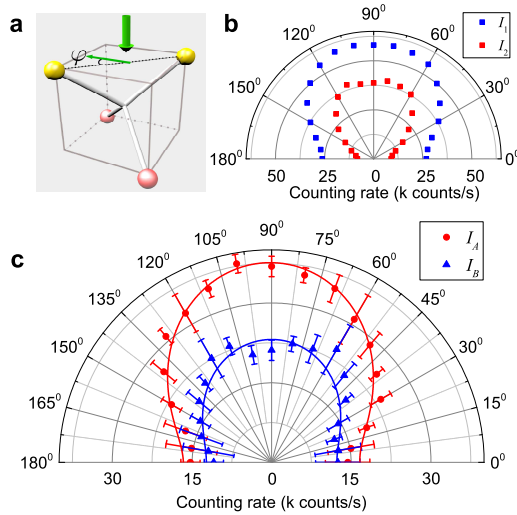


FIG. 5: (color online) (a) The schematic of two sets of axes for [100]-oriented NV center sample according to the polarization of pump beam. They are in the plane of $\varphi = 0^\circ$ or $\varphi = 90^\circ$. (b) Single-photon and two-photon emission intensity versus the polarization angle of pump beam. The two-photon intensity was amplified by 5×10^3 for view. (c) Separated intensities of two NV centers versus the polarization angle of pump beam.

ters cannot be readily distinguished by the classical method [18]. Here, the resolution (see Supplementary for details) was determined by the number of recorded photons and the experimental setup. In the present measurement, the error is about 0.9 nm with 10^5 coincident photon counts and the setup repeat resolution for x or y axis is about 0.7 nm.

Besides the images of nearby particles, such a quantum measurement method can be easily generalized to measure and distinguish other properties even with high overlapping. For example, the axes of the NV centers can be measured. The spontaneous emission rates vary with the polarization of the pump beam according to different axes of NV centers [28, 29]. With polarized optical pump for our [100]-oriented sample, number of possible orientations of a given center is reduced from four to two, which are in the plane of $\varphi = 0^\circ$ or $\varphi = 90^\circ$ as shown in Fig. 5 (a). However, it is difficult to get the information of the axes optically if the two NV centers are deep within diffraction limit. Here with QSI, the axes of the pair of NV centers at the distance of 8.5 nm have been obtained. With different polarized pump beam, the single-photon and two-photon counts are measured and showed in Fig. 5 (b). Simply, the emission intensity of each NV centers with the angle of polarization can be obtained, as shown in Fig. 5 (c). Correspondingly, the axes of the two NV centers are same in the plane of $\varphi = 0^\circ$. The data can be fitted with $I_{A(B)} = \alpha_{A(B)} + \beta_{A(B)} \cos^2 \varphi$ [29] with $\alpha_{A(B)} = 37.5 \pm 0.4 (23.1 \pm 0.5)$ and $\beta_{A(B)} = -21.0 \pm 0.8 (-10.8 \pm 0.9)$. The small dip at $\varphi = 90^\circ$ for NV_B may come from its depth in the diamond [28].

In summary, a practical QSI method was demonstrated

based on the unique quantum behavior of anti-bunching emission photons. Two well-overlapping NV centers can be spatially resolved. Also, the axes of the two NV centers are measured even their distance is within 8.5 nm. Compared to other image methods, the experimental setup for QSI is simple. It does not need complicated pump beams [18, 22] or the assistance of other control systems [18, 19]. With a high order of coincident multi-photon measurements, additional single NV centers can be imaged and distinguished. The QSI method can be applied to detect and distinguish images with random continuous envelopes, in addition to the demonstrated symmetric envelopes of the photons from the NV centers. Furthermore, the QSI method can be used to distinguish other degrees of freedom that are overlapping, such as lifetime, frequency, and polarization. The QSI method is also suitable for the detection of other particles, such as atoms, quantum dots, and molecules. Because the photons from each quantum particle can be recorded and simultaneously distinguished without decoupling nearby quantum particles, the QSI method can be used to detect their separate dynamics, as well as the coupling between them. The scalable QSI with high order coincidence counts will be applied in the multipartite interaction for quantum information techniques and modern physics.

This work was supported by the 973 Programs (No.2011CB921200 and No. 2011CBA00200), the National Natural Science Foundation of China (NSFC) (No. 11004184), the Knowledge Innovation Project of the Chinese Academy of Sciences (CAS), and the Fundamental Research Funds for the Central Universities.

* Electronic address: fwsun@ustc.edu.cn

- [1] P. Alivisatos, *Nature Biotechnol.* **22**, 47 (2004).
- [2] G. Patterson, M. Davidson, S. Manley, and J. Lippincott-Schwartz, *Annu. Rev. Phys. Chem.* **61**, 345 (2010).
- [3] E. A. Ash, and G. Nicholls, *Nature* **237**, 510 (1972).
- [4] W. Denk, J. H. Strickler, and W. W. Webb, *Science* **248**, 73 (1990).
- [5] T. A. Klar and S. W. Hell, *Opt. Lett.* **24**, 954 (1999).
- [6] M. J. Rust, M. Bates, and X. Zhuang, *Nature Meth.* **3**, 793 (2006).
- [7] E. Betzig, *et. al.*, *Science* **313**, 1642 (2006).
- [8] S. T. Hess, T. P. Girirajan, and M. D. Mason, *Biophys. J.* **91**, 4258 (2006).
- [9] T. Dertinger, R. Colyer, G. Iyer, S. Weiss, and J. Enderlein, *Proc. Natl. Acad. Sci. USA* **106**, 22287 (2009).
- [10] V. Giovannetti, S. Lloyd, and L. Maccone, *Science* **306**, 1330 (2004).
- [11] The LIGO Scientific Collaboration, *Nature Phys.* **7**, 962 (2011).
- [12] T. Nagata, R. Okamoto, J. L. O'Brien, K. Sasaki, and S. Takeuchi, *Science* **316**, 726 (2007).
- [13] F. W. Sun, B. H. Liu, Y. X. Gong, Y. F. Huang, Z. Y. Ou, and G. C. Guo, *EPL* **82**, 24001 (2008).
- [14] G. Y. Xiang, B. L. D. Higgins, W. H. Berry, M. G. Wiseman, and J. Pryde, *Nature Photon.* **5**, 43 (2011).
- [15] H. J. Kimble, M. Dagenais, and L. Mandel, *Phys. Rev. Lett.* **39**, 691 (1977).

- [16] C. Kurtsiefer, S. Mayer, P. Zarda, and H. Weinfurter, Phys. Rev. Lett. **85**, 290 (2000).
- [17] T. M. Babinec, *et. al.*, Nature Nanotech. **5**, 195 (2010).
- [18] P. C. Maurer, *et. al.*, Nature Phys. **6**, 912 (2010).
- [19] P. Neumann, *et. al.*, Nature Phys. **6**, 249 (2011).
- [20] Y. -R. Chang, *et. al.*, Nature Nanotech. **3**, 284 (2008).
- [21] L. P. McGuinness, *et. al.*, Nature Nanotech. **6**, 358 (2011).
- [22] E. Rittweger, D. Wildanger, and S. W. Hell, EPL. **86**, 14001 (2009).
- [23] A. Gruber, *et. al.*, Science **276**, 2012 (1997).
- [24] C. Santori, D. Fattal, J. Vučković, G. S. Solomon, and Y. Yamamoto, Nature **419**, 594 (2002).
- [25] F. W. Sun and C. W. Wong, Phys. Rev. A **79**, 013824 (2009).
- [26] O. Schwartz and D. Oron, Phys. Rev. A **85**, 033812 (2012).
- [27] R. Hanbury Brown and R. Q. Twiss, Nature **177**, 27 (1956).
- [28] R. J. Epstein, F. M. Mendoza, Y. K. Kato, and D. D. Awschalom, Nature Phys. **1**, 94 (2005).
- [29] T. P. M. Alegre, C. Santori, G. Medeiros-Ribeiro, and R. G. Beausoleil, Phys. Rev. B **76**, 165205 (2007).